Research Square

Preprints are preliminary reports that have not undergone peer review.
They should not be considered conclusive, used to inform clinical practice,
or referenced by the media as validated information.

Astragalin Ameliorates Cognitive Dysfunction Through Inhibiting PI3K/Akt-MTOR-Mediated Autophagic Flow in Hippocampal Neurons of APP/PS1 Mice

Cuizhu Yang
Guangdong Pharmaceutical University
Runheng Zhang
Guangdong Pharmaceutical University
Shuhan Wang
Guangdong Pharmaceutical University
Yinghong Tian
Southern Medical University
Yaqi Yang
Guangdong Pharmaceutical University
Jing Liu
Guangdong Pharmaceutical University
YUXIN MA (myx117@163.com)
Guangdong Pharmaceutical University https://orcid.org/0000-0002-6213-6208

Research Article

Keywords: Alzheimer's disease (AD), Astragalin (AST), autophagy, autophagic flow, PI3K/Akt-mTOR, APP/PS1 mice.

Posted Date: January 5th, 2022

DOI: https://doi.org/10.21203/rs.3.rs-1209539/v1

License: This work is licensed under a Creative Commons Attribution 4.0 International License.
Read Full License

Abstract

Astragalin (AST), a natural small molecule flavonoid, can exert anti-oxidant, anti-inflammatory and anti-cancer impacts by regulating autophagy. However, the potential mechanism of the neuroprotective effect of AST on neurological disorders such as Alzheimer's disease (AD) is still not clear. In the present study, we firstly screened AST for the treatment of AD from the ingredients of Chinese medicines such as Acori tataninowii Rhizoma, Eucommiae Cortex, Paeoniae Radix Alba through the traditional Chinese medicine systems pharmacology database and analysis platform (TCMSP) database. And then we found that AST could improve the cognitive abilities of APP/PS1 mice by Step-down passive avoidance (SDA) and Morris Water Maze (MWM) Test. Further, we identified that AST diminished Aβ plaques deposition in the brains of APP/PS1 mice and Aβ as well as Aβ42 levels in the serum of APP/PS1 mice. Next, microtubule-associated protein 1 light chain 3B (LC3B), p62, Beclin-1, ATG5, ATG12, LAMP-1 were observed to be co-expressed with NeuN in the hippocampus of APP/PS1 mice by immunofluorescent multiplex staining, while AST was able to activate autophagy and maintain autophagic flow in hippocampal neurons of APP/PS1 mice by western blot (WB) analysis. Finally, AST reduced the expressions of p-PI3K, p-Akt, p-mTOR by WB analysis. Taken together, we confirmed that AST may play key neuroprotective effects on APP/PS1 mice by inhibiting the PI3K/Akt-mTOR signaling pathway to activate autophagy and keep autophagic flow smooth.

Introduction

Alzheimer's disease (AD) is a neurodegenerative disorder characterized by memory loss and progressive cognitive dysfunction [1, 2]. According to the latest statistics of AD Research Association, the number of deaths caused by AD has exceeded the total number of patients with breast cancer and prostate cancer, ranking first in the world [3]. In contrast, about 9.83 million people aged ≥ 60 years in China suffer from AD [4]. The prevalence and incidence of AD are increasing year by year, and at present, AD has become the most common disease that endangers the health of the elderly. So far, the pathogenesis of AD is not thoroughly understood, and therefore there is still a lack of effective drugs for targeted therapy according to AD in clinical practice. Therefore, finding valid strategies and drugs for prevention and treatment AD is of vital importance.

As a degradation mechanism, autophagy is the process of removing damaged and aging organelles, which is essential for maintaining cell homeostasis in the brain [5]. The deficits of autophagy bring about the pathogenesis of numerous neurodegenerative diseases, including AD [6]. Mounting evidences suggest that AD is accompanied with autophagy dysfunction, resulting in the abnormal accumulation of Aβ plaques that cannot be degraded in the brain, and the regulation of autophagy can facilitate the clearance of Aβ plaques [7–9]. Autophagic flux which means the integrate process of autophagy, includes autophagy initiation, autophagosome formation, autolysosome fusion and degradation [10], while abnormalities in any of the above links can cause the excessive aggregation of Aβ plaques [11]. Thus, we evaluated all the primary steps of the autophagic process to estimate the influence of the autophagic flux on the pathological development of AD.

Astragalin (AST), as a natural small molecule flavonoid compound [12], is widely distributed in various medicinal plants and fruits, such as Eucommia cortex, lotus leaf and persimmon [13–15]. Currently, increasing evidences have verified AST can be used as a prescription of traditional Chinese medicine owing to its anti-inflammatory [16], anti-cancer [17], and anti-oxidant [18] effects by regulating autophagy. However, whether AST can ameliorate neurological diseases such as AD by modulating autophagy has not yet been reported in related in vivo studies. Consequently, we conducted this experiment to examine the crucial impact of AST on cognitive function of AD mouse models and the autophagy-related mechanism of eliminating Aβ plaques in the brain, and so as to provide animal experiment and theoretical basis for AST as a potential clinical drug for the treatment of AD.

Materials And Methods

Animals and treatment

A total of 28 male 8-week-old APP_{Swe}, $PSEN1_{dE9}$ transgenic mice and 7 male C57BL/6 (WT-like littermates) mice were obtained from Guangdong Medical Laboratory Animal Center, China (Permit Number: SCXK GUANGDONG 2018-0002). The APP/PS1 transgenic mice were reared in a single cage, and all the animals were housed under a standard condition of an even dark/light cycle at 25 ℃. After adapting to the environment for one week, the APP/PS1 transgenic mice were randomly divided into: the APP/PS1 group, 10 mg/kg AST (APP/PS1+AST 10) group, 20 mg/kg AST (APP/PS1+AST 20) Group, 40 mg/kg AST (APP/PS1+AST 40) group, and the C57BL/6 mice were served as the WT group. AST was freshly prepared in dimethyl sulfoxide (DMSO) to make working solutions at concentrations of 10, 20 and 40 mg/kg [19, 20]. Subsequently, these mice were administrated orally with AST treatment once daily for one month. The mice of WT group and APP/PS1 group were gavaged with an equal volume of saline configuration of 0.1% DMSO. All experimental protocols in this study were approved by the Ethics Committee of Guangdong Pharmaceutical University and were complied with the National Institutes of Health Guide for the Care and Use of Animals.

Materials, antibodies and reagents

AST (B21704) with a purity of 98% were purchased from YuanYe Bio-Technology Co., Ltd. (Shanghai, China); rabbit anti-p-mTOR (5536S), rabbit anti-mTOR (2983S), rabbit anti-p-Akt (4060S) and rabbit anti-Akt (4691S) were purchased from Cell Signaling Technology, Inc. (Danvers, MA); p-PI3K (ab191606), rabbit anti-PI3K (ab182651), rabbit anti-LC3B (ab51520), rabbit anti-SQSTM1/p62 (ab91526), rabbit anti-Beclin-1 (ab217179), rabbit anti-ATG5 (ab108327), rabbit anti-ATG12 (ab155589), rabbit anti-LAMP-1 (ab62562), mouse anti-NeuN (ab104224), rabbit anti-β-Actin (ab8227), rabbit anti-GAPDH (ab181602), Goat anti-rabbit IgG H&L (Alexa Fluor® 488) (ab150077), Goat anti-mouse IgG H&L (Alexa Fluor® 594) (ab150116) and Goat anti-rabbit IgG H&L (HRP) (ab205718) were purchased from Abcam (Cambridge, MA). The mouse anti-beta amyloid (1-42) (GT622) was obtained from GeneTex (Southern California, USA); ELISA kit for mouse Aβ was purchased from Jiangsu Meimian industrial Co., Ltd (Jiangsu, China). ELISA kit for mouse Aβ42 was bought from Wuhan Fine Biotech Co., Ltd (Wuhan, China). The

chemiluminescence imaging and analysis system was purchased from Shanghai Tanon Technology Co., Ltd (Shanghai, China) and the fluorescence microscope was purchased from the Olympus Company (Tokyo, Japan).

Step-down passive avoidance (SDA) test

Before and after the administration, all animals were subjected to the SDA test. The SDA test was used to assess the learning and memory of rodents [21, 22]. The experimental device was composed of an avoidance reaction box (15×15×46 cm^3) and a parallel steel rod with energization at the bottom. A circular insulating platform (4.5 cm in a diameter, 4.5 cm in a height) was placed in the middle of the box. The mice of each group were put into the reaction box to adapt to the environment for 3 min, and then electrified. The mice were stimulated by the electric current (36 V, 0.5 mA, 5 min) and jumped back to the platform to avoid noxious stimulation. Animals were trained for 3 consecutive days and the experiment was formally started after 24 h. The retention of memory was assessed by measuring the time when the mice firstly stepped down the platform (step down latency) and the number of times the mice jumped off the platform within 5 min (number of errors). The schedule of SDA test is shown in Fig. 1.

Morris Water Maze (MWM) Test

Before and after the treatment of AST, the MWM behavioral experiment was conducted to evaluate the spatial memory and learning and memory abilities of mice [23]. The MWM includes a mouse behavior test system, an image automatic monitoring and processing system, and a data processing analysis system. Tests were carried out in a circular tank (120 cm diameter and 40 cm deep) containing opaque water maintained at 25 ± 2°C. Tests include positioning navigation test, space exploration test and visible platform test. All mice were subjected to a 5-day hidden platform test and were regularly trained 4 times a day. Removing the platform on day 6, the mice were placed in the water from the same quadrant and then the time of mice reaching the original platform quadrant within 1min were recorded. On day 7 and 8, the platform was raised to a position 1 cm above the water surface and placed in the other quadrant, and then the swimming track and the times of mice crossing the target platform quadrant within 1 min were recorded. The schedule of MWM test is shown in Fig. 1.

Fluorescent imaging of Aβ plaque in the brain of mice

After completing drug treatment and behavioral studies, the mice were anesthetized and perfused with 4% paraformaldehyde (PFA) through the aorta, and then brain tissues were taken out for fixation and washed with flowing water. After gradient dehydration, paraffin embedding and tissue sectioning, the brain sections of mice in each group were selected for routine dewaxing and dehydration. Then 0.01 M citrate buffer (PH: 6.0) was used to antigen retrieval at high-temperature for 20 min. After blocking the binding site of non-specific antibody, mouse anti-Aβ1-42 (1:300) was incubated overnight at 4°C. Then the sections were washed by PBST and Goat anti-mouse IgG H&L (Alexa Fluor® 594) (1:800) was added and incubated at 37°C for 1 h. After washing by PBST, the sections were dyed in 0.3% thioflavin S solution for 15 min, and then washed in 70%, 50% I and 50% II ethanol solutions for 5 min. Next, 50%

glycerol was used for sealing [24]. Sections were observed by a fluorescent microscope. Image J (NIH, Bethesda, MD, USA) software was used to determine the number of plaques.

Determination of Aβ and Aβ42 in the serum of mice by ELISA

To detect Aβ and Aβ42 levels in serum of mice, the blood of mice was collected before sacrificing mice. The serum was then separated by centrifugation at 1000 rpm for 10 min at 4℃. Subsequently, the levels of Aβ and Aβ42 in serum of mice were measured by mouse Aβ ELISA kit and mouse Aβ42 ELISA kit. At last, the absorbance A under 450 nm wave was measured by microplate reader, and the samples concentration were calculated by Curve Expert 1.4 (Hyams DG, Starkville, MS, USA).

Immunohistochemistry

The brain sections were dewaxed and dehydrated with xylene and ethanol solution. Then sections were repaired with 0.01 M citrate buffer (PH: 6.0) at high-temperature for 20 min. After blocking the binding site of non-specific antibody, rabbit anti-LC3B (1:600), rabbit anti-SQSTM1/p62 (1:100), rabbit anti-Beclin-1 (1:200), rabbit anti-APG5L/ATG5 (1:250), rabbit anti-ATG12 (1:200), rabbit anti-LAMP-1 (1:300) and mouse anti-NeuN (1:500) were added and incubated overnight at 4°C. Sections were then washed by PBST and Goat anti-rabbit IgG H&L (Alexa Fluor 488) (1:800) and Goat anti-mouse IgG H&L (Alexa Fluor 594) (1:800) were added and incubated at 37°C for 1 h. After washing by PBST, the sections were dripped with the anti-fluorescence quencher containing DAPI. Then the coverslips were taken out for sealing. The sections were observed by a fluorescent microscope. Image J software was used to analyze the fluorescent intensity.

Western blot

After the mice were anesthetized, their hippocampal tissues were removed by decapitation and placed in RIPA lysis buffer containing phenylmethylsulfonyl fluoride (PMSF). Next, these tissues were fully ground on ice and transferred to centrifuge tubes, and then the supernatant was collected after high-speed centrifugation at 4℃. The Pierce BCA Protein Assay kit was used to determine the protein content of tissues, followed by electrophoresis, membrane transfer, and then the following primary antibodies were added respectively after blocking nonspecific sites: rabbit anti-PI3K (1:1000), rabbit anti-p-PI3K (1:2000), rabbit anti-Akt (1:2000), rabbit anti-p-Akt (1:1000), rabbit anti-mTOR (1:1000), rabbit anti-p-mTOR (1:1000), rabbit anti-LC3B (1: 3000), rabbit anti-p62 (1: 2000), rabbit anti-Beclin-1 (1: 500), rabbit anti-APG5L/ATG5 (1:1000), rabbit anti-ATG12 (1:2000), rabbit anti-LAMP-1 (1:1000), rabbit anti-GAPDH (1:10000) and rabbit anti-β-actin (1: 3000), which were incubated overnight at 4℃. Then HRP-labeled goat anti-rabbit IgG (1: 8000) or HRP-labeled goat anti-mouse IgG (1: 3000) were incubated for 80 min at room temperature. Subsequently, the automatic chemiluminescence imaging and analysis system was used to measure bands. The optical density of each protein band was quantified using Image J software.

Bioinformatics analysis

The traditional Chinese medicine systems pharmacology database and analysis platform (TCMSP) (https://old.tcmsp-e.com/tcmsp.php) database was searched to obtain the chemical compositions of the therapeutic AD herbs, and then aggregated into a table. The tested gene proteins were imported into the String Gene Interaction Network database (https://string-db.org/) and the species was selected as “Homosapiens”. The selected targets were searched in “Multiple proteins” and the PPI network map was drawn.

Statistical analysis

All experiments were repeated at least three times. And all the experiments included a minimum of three mice per group. Graphpad Prism 8.0 (GraphPad Software Inc., California, USA) and SPSS 23.0 software (IBM, Armonk, NY, USA) were used to analyze these data. All of the data were expressed as mean ± standard deviation (SD). Quantitative data meet the normal distribution, and after passing the homogeneity test of variance, one-way ANOVA or two-way ANOVA was used to compare groups followed by Turkey or Student-Newman-Keuls test. For comparison between two groups, statistical significance was determined by two-tailed unpaired *t*-test. And the $P < 0.05$ was considered to be significant.

Results

AST exists in most Chinese herbal medicines for the treatment of AD

Firstly, we used the TCMSP database and set the screening condition to the drug-like property (DL) ≥ 0.18, which yielded that among the Chinese herbal medicines used in the treatment of AD, Acori tataninowii Rhizoma [25], Eucommiae Cortex [26], Paeoniae Radix Alba [27], Carthami Flos [28], Forsythiae Fructus [29], Achyranthis Bidentatae Radix [30], Granati Pericarpium [31], and Epimrdii Herba [32] contained AST (Table 1).

Table 1
Part of the components of Chinese herbal medicines for the treatment of AD

Traditional Chinese medicine (TCM)	Partial Molecule Name
Acori tataninowii Rhizoma	8-Isopentenyl-kaempferol, Cycloartenol, beta-asarone, eugenol, Astragalin
Eucommiae Cortex	protocatechuic acid, vanillic acid, LOLIOLIDE, Trochol, genipin, Astragalin
Paeoniae Radix Alba	propyl (2R)-2-hydroxypropanoate, gallotannin, paeonoside, Astragalin
Carthami Flos	o-xylene, p-xylene, l-Verbenone, Nonanal, Arachic acid, Decanal, Astragalin
Forsythiae Fructus	vanillic acid, Cymol, citral, (-)-alpha-Pinene, (-)-nopinene, CAM, Astragalin
Achyranthis Bidentatae Radix	poriferasta-7,22E-dien-3beta-ol, chikusetsusaponin □a, 3-epioleanolic acid, Astragalin
Granati Pericarpium	Officinalisin, Punicalin, 1-Methyl-3-isopropoxy cyclohexane, Astragalin
Epimrdii Herba	(L)-alpha-Terpineol, dec-2-enal, copaene, isoliquiritigenin, DFV, Astragalin

Learning and cognitive dysfunction in the APP/PS1 mice

Firstly, we evaluated the cognitive deficits related to AD by using the SDA test and MWM test, and then selected APP/PS1 mice needed for this experiment (Fig. 2a, b). In the SDA test, it was observed that the APP/PS1 mice showed shorter step-down latency (time to jump off the platform for the first time) than WT mice (p<0.001, Fig. 2c,). Meanwhile, the number of errors made by APP/PS1 mice were much higher than that of WT mice (p<0.001, Fig. 2d).

The MWM results showed that the escape latency (time to find the target platform) of APP/PS1 mice was significantly longer than WT mice during the hidden-platform period, especially from Day 5 (p<0.001, Fig. 2e). During the space exploration test, APP/PS1 mice took much longer time to visit the target quadrant compared with WT mice (p<0.001, Fig. 2f). After the platform was raised to 1 cm above the water surface, it was observed that the times of APP/PS1 mice crossing the quadrant of the target platform were significantly less than WT mice (p<0.001, Fig. 2g, h). Together, the above results indicated that APP/PS1 mice had learning, memory and cognitive dysfunction.

AST treatment ameliorates cognitive impairments of APP/PS1 mice

Next, to explore whether AST could improve the cognitive deficits of APP/PS1 mice, we conducted the SDA test and MWM test once again. The results of the SDA test showed that compare with WT mice,

APP/PS1 mice had a shorter step-down latency and an increase in the number of errors (p<0.001, Fig. 3a, b), while these changes were reversed after treatment with 20, 40 mg/kg AST (p<0.01, Fig. 3a, b).

In MWM test, during the training period the APP/PS1 mice showed much longer escape compared with WT mice, while AST significantly reduced the escape latency of APP/PS1 mice, especially from Day 5 (p<0.001, Fig. 3c). During the trial period, the APP/PS1 mice spent significantly much longer time to find the target quadrant and reached the target platform much less frequently when compared with the WT mice and the mice treated with AST (p<0.01, Fig. 3d, e, f). In summary, the results revealed that AST significantly improved the cognitive deficit of APP/PS1 mice.

AST treatment reduces Aβ accumulation of APP/PS1 mice

In the following, we evaluated Aβ plaques deposition in the brain of APP/PS1 mice after treatment with different doses of AST drugs. As shown in the Fig. 4a, compared with WT mice, there were a large amount of the depositions of Aβ plaque in the brain of APP/PS1 mice (p<0.001, Fig. 4a, b). However, after treatment with AST, Aβ plaques were considerably reduced in a dose-dependent manner, especially after treatment with 40 mg/kg AST (p<0.001, Fig. 4a, b).

Then we further assessed the impacts of AST on the levels of soluble and insoluble Aβ and Aβ42 in the serum of mice by using ELISA assay. By contrast with WT mice, Aβ and Aβ42 levels in the serum of APP/PS1 mice were more higher (p<0.001, Fig. 4c, d). While after being treated with 20 and 40 mg/kg AST for one month, Aβ and Aβ42 levels in serum of APP/PS1 mice were decreased (p<0.01, Fig. 4c, d).

AST treatment activates autophagy in APP/PS1 mouse hippocampal neurons

By considering that AST treatment could attenuate cognitive function and Aβ plaques deposition of mice, we next investigated whether AST-mediated effects could regulate autophagy and autophagic flux. Firstly, we detected the levels of LC3B, p62 and Beclin-1 involved in the initiation of autophagy by immunofluorescent staining and WB analysis. The results of immunofluorescence showed that LC3B positive cells were mainly located in the cytoplasm of mice hippocampal neurons (Fig. 5a), p62 positive cells were mainly located in the in the cytoplasm and nucleus of mice hippocampal neurons (Fig. 5b), and Beclin-1 positive cells were mainly located in the cytoplasm and membrane of mice hippocampal neurons (Fig. 5c). The levels of LC3B and Beclin-1 in APP/PS1 mice hippocampus were lower than those in WT group, while the level of p62 was higher (p<0.01, Figure 5d, e, f). Notably, treated with AST, the levels of LC3B and Beclin-1 increased to varying degrees, while the p62 level decreased in a different degree (p<0.05, Fig. 5d, e, f). Among them, the 40 mg/kg AST treatment was the most obvious (p<0.01, Figure 5d, e, f). Collectively, all abovementioned results showed that AST treatment activated autophagy of hippocampal neurons in APP/PS1 mice.

AST treatment promotes autophagosome formation and autophagolysosome degradation in hippocampal neurons

of APP/PS1 mice

Next, immunofluorescent staining and WB assays were performed in hippocampal of mice to detect the expressions of ATG5 and ATG12 related proteins involved in autophagosome formation. As shown in the Fig. 6: ATG5 positive cells were mainly located in the cytoplasm of mice hippocampal neurons (Fig. 6a), and ATG12 positive cells were mainly located in the cytoplasm of mice hippocampal neurons (Fig. 6b). The similar phenomenons were found ATG5 and ATG12 in the hippocampus of the APP/PS1 group were obviously lower than those in WT group (p<0.01, Fig. 6d, f, g). Meanwhile, with the AST treatment, the ATG5 and ATG12 were efficiently upregulated in a dose-dependent manner, among which treated with 40 mg/kg AST was especially meaningful (p<0.01, Fig. 6d, f, g). Taken together, the results indicated that AST treatment could promote the formation of autophagosomes in the hippocampal neurons of APP/PS1 mice.

Finally, to further investigate the impact of AST on the degradation of autophagy lysosomes, we also inspected the level of lysosomal membrane protein LAMP-1 by immunofluorescence and WB assays. As indicated in Fig. 6c, LAMP-1 positive cells were mainly located in the cell membrane of mice hippocampal neurons (Fig. 6c). Compared with the WT mice, the level of LAMP-I protein in the hippocampus of APP/PS1 mice was decreased significantly (p<0.01, Fig. 6e, h). In contrast, while the treatment with 10, 20 and 40 mg/kg AST enhanced the level of LAMP-I protein, among which 40 mg/kg AST showed the most obvious effect (p<0.001, Fig. 6e, h). Together, the above results demonstrated that AST treatment promoted the degradation of autophagy lysosomes in hippocampal neurons of APP/PS1 mice.

PI3K/Akt-mTOR is involved in the neuroprotective effect of AST on APP/PS1 mice

The PI3K/Akt-mTOR pathway plays various important roles in the central nervous system and is closely related to the pathogenesis of AD [33]. Therefore, we firstly used STRING for protein interaction network analysis and found that PI3K/Akt-mTOR pathway-related proteins were interacted with related proteins that regulated autophagic flow (Fig. 7a) (Source: 9 items (mouse) - STRING interaction network (string-db.org)). In order to evaluate whether AST could regulate these proteins to ameliorate the pathological behavior of APP/PS1 mice, we then used WB to detect the proteins expression and phosphorylation forms of PI3K, Akt, and mTOR. As shown in the Fig. 7, p-PI3K, p-Akt and p-mTOR in the hippocampus of APP/PS1 mice were significantly increased with a varied degree compared to those in the WT mice (p<0.01, Fig. 7b, c, d, e). Consistent with expectations, treated with AST, the expressions of p-PI3K, p-Akt and p-mTOR in the hippocampus of APP/PS1 mice were distinctly reduced, especially when treated with 40 mg/kg AST (p<0.01, Fig. 7b, c, e), suggesting that the PI3K/Akt-mTOR signaling pathway was inhibited after AST treatment.

Discussion

In the present study, we demonstrated the learning and memory functions were impaired in APP/PS1 mice by SDA and MWM behavioral experiments. Subsequently, we inquired the TCMSP database to ascertain that most of the Chinese medicines used to treat AD contained AST. Based on this discovery, we intraperitoneal injection of AST in APP/PS1 mice for one month noticed that AST treatment productively accelerated the clearance of Aβ plaque deposits in the brains of APP/PS1 mice and further restored their cognitive dysfunction. Importantly, we revealed AST could active autophagy and keep autophagic flow smooth of APP/PS1 mice hippocampal neurons for neuroprotective effect by inhibiting PI3K/Akt-mTOR pathway (Fig. 8). The above findings indicate AST might be a potential trerapeutic agent for future clinical AD treatment.

AD, as a common progressively neurodegenerative disorder, endangers the memory and cognitive abilities of people around the world [34, 35]. As the universal animal model of AD, APP/PS1 mice stably display mouse/human APP located in neurons and mutant human PS1 and there are senile plaque deposits in the brain at the age of 6 months, and memory ability decline with age [36]. Our data in this study manifested that APP/PS1 mice had severe memory deterioration, which is consistent with several related researches [37–39]. The brains in AD showing excessive senile plaque depositions are extensively regarded as one of the earliest changes [40]. Concurrently, we observed that, dissimilar to WT mice, there were numerous Aβ plaque deposits in the brain of APP/PS1 mice. Interestingly, we found the contents of Aβ and Aβ1-42 which were the most common and toxic [41, 42] in the blood of APP/PS1 mice were much higher than those of WT mice. Hence, inhibiting the aggregation of Aβ and reducing the content of Aβ and Aβ1-42 in the serum of mice may be a hopeful treatment strategy for AD.

Currently, traditional Chinese medicines play an indispensable performance in the prevention and treatment of AD in domestic and international studies. Thus, we screened out AST, a potential new natural flavonoid isolating from traditional Chinese medicines for AD treatment [43], by consulting a large amount of literatures and operating the TCMSP database. In the central nervous system, AST further exerted a good hypnotic effect by prolonging the convulsion latency and diminishing the convulsion rate of mice [44]. Concurrently, AST showed neuroprotective impact on PC12 cells and SH-SY5Y by enhancing cell viability and weakening intracellular oxidative stress [45]. Additionally, the experimental evidence of Chung et al. proved that AST could prevent H2O2-induced cell death by inhibiting JNK, p38 and ERK 1/2 pathways in SK-N-SH cell [46]. However, studies on the function of AST in neurodegenerative diseases such as AD are comparatively less frequent and solely concentrated on the cell levels in vitro. In the previous investigation of AD in vitro, it has been reported that AST could shorten the intracellular tau protein level and alleviate the cell damage through pharmacological analysis [47]. Here, we administered AST to APP/PS1 mice and primarily confirmed that AST was validly in recovering impaired cognitive functions in APP/PS1 mice, including learning and memory and spatial navigation. Subsequently, we were surprised to discover that abundant and widespread Aβ plaques in the brains of APP/PS1 mice were productively abolished, as well as Aβ and Aβ1-42 levels in the serum of mice. Notably, the therapeutic effect of 40 mg/kg AST treatment was the most visible in this process. In line with those, we further discussed the relevant mechanisms of AST on the neuroprotective infection of APP/PS1 mice.

From early to late AD, the autophagy of hippocampal neurons is continuously disrupted and the process of autophagic flow is blocked, bringing about the inefficiency to eliminate the pathogenic Aβ plaques accumulated in the cytoplasm, thus exhibiting high toxicity to cells [48–50]. Revamping hippocampal neuronal autophagy functional impairment may be of indispensable significance in postponing aging and hampering neurodegenerative diseases such as AD [51]. In the present research, we revealed NeuN, a labeled neuronal protein, was co-expression with autophagy-related proteins involved in the whole autophagic flow by immunofluorescent multiple staining experiments, which further suggested the presence of autophagy in mouse hippocampal neurons. LC3B presents in autophagosomes in the form of LC3B-Ⅰ and LC3B-Ⅱ, while the level of the lapidated form of LC3B-Ⅱ is a factual measure of autophagic flux relative to the unprocessed LC3B-Ⅰ [52, 53]. SQSTM1/p62 is a ubiquitin-binding protein that can be efficiently degraded by autophagy, and thus, the level of p62 is another indicator of autophagic flux [54, 55]. The WB analysis demonstrated that LC3B-II levels in hippocampal neurons of APP/PS1 mice were much lower than those of WT mice, whereas p62 levels showed the opposite trend, which could be the result of blocked autophagic flow pathways. Importantly, the two changes were reversed again with treatment of 20 and 40 mg/kg AST, indicating that autophagy was activated. Owing to autophagic flow is a dynamic process, as a meaningful protein for autophagy initiation, Beclin-1 mediates the positioning of other autophagic proteins, and its increased levels indicate autophagic activation [56]. Here, we determined AST predominantly enhanced the decreased Beclin-1 levels coincided with the ability of AST to ensure that the autophagic flow initiation phase was normalized again in the hippocampus of APP/PS1 mice. ATG5 gene exerts an imperatively character in the extension of autophagosomal membrane as well as autophagosome formation [57]. Meanwhile, the role of ATG12, an essential gene of the ATG12-ATG5 coupling system, can not be underestimated [58]. In this study, ATG5 and ATG12 in the hippocampus of APP/PS1 mice shifted expeditiously from lower to higher after AST treatment, in a sense revealing that AST established the proper functioning of the intermediate link of autophagic flow (autophagosome formation phase). The inability of autophagosomes to fuse with lysosomes to further form autophagic lysosomes, which in turn break down harmful substances, can also lead to serious consequences [59]. The reduction of LAMP-1 (a lysosomal membrane-bound protein that works in autophagic lysosome fusion) in our study indicated that autophagic lysosome formation was arrested in the hippocampus of APP/PS1 mice [60–62]. Novertheless, AST bolstered the fusion of autophagosomes with lysosomes by extending LAMP-1 level, thereby accelerating the clearance of toxic substances in the brain of APP/PS1 mice. The above results indicated in the APP/PS1 mice hippocampal neurons AST could active autophagy and keep autophagic flow smooth by stimulating the degradation of p62, augmenting the formation of LC3B and Beclin-1, up-regulating ATG5, ATG12 and LAMP-I.

We hypothesized that AST upregulated the level of autophagy and controlled autophagic flow in the hippocampus of APP/PS1 mice by restraining the PI3K/Akt-mTOR pathway. mTOR as known to be the major negative regulator of autophagy, is monitored by PI3K/Akt kinase cascade response, and when it is inhibited, the autophagic activity is enhanced [63, 64]. Numerous researches have shown that superfluous activation of the PI3K/Akt-mTOR signaling pathway made for the inhibition of neuronal autophagy level and the inability to clear intracellular accumulation of Aβ and tau proteins in a timely manner, which to

some extent aggravated amyloid plaque production and neurofibrillary tangles in the AD brains [33, 65]. In contrast, inhibition of PI3K/Akt-mTOR pathway was able to scale down Aβ aggregation and improve cognitive function of AD mice [66, 67]. In our study, equivalently, above mentioned pathway was aberrantly mobilized in the hippocampus of APP/PS1 mice compared to normal mice, whereas AST stimulated autophagy and sustained either process of autophagic flow unimpeded by inhibiting the PI3K/Akt-mTOR pathway.

In conclusion, our study demonstrated that AST could exert the partial neuroprotective effect on APP/PS1 mice by facilitating PI3K/Akt-mTOR-mediated autophagy flux pathway. And our data provides more theoretical support for the application of AST to clinical AD effective drug candidates. However, in the current study we didn't clearly clarify which key link autophagic flux was regulated by AST to exert neuroprotective effects. Therefore, we need to explore it further in the future.

Declarations

Funding

This experimental procedures were supported by the Natural Science Foundation of Guangdong Province (No. 2018A0303130073), and the Pearl River S&T Nova Program Foundation of Guangzhou City of China (No. 201710010002).

Compliance with Ethical Standards

This work was supported by the Ethics Committee of Guangdong Pharmaceutical University (Guangzhou, China: Approval No. : SPF-2017356).

Conflict of Interest

All authors of this article claimed they had no conflict of interest.

Consent to Participate

Not applicable.

Consent for Publication

All authors consent to the publication of this manuscript.

Availability of data and materials

All data and materials used in this study are available from the corresponding authors upon reasonable request.

Authors' contributions

Yuxin Ma and Cuizhu Yang designed the study and wrote the paper. Cuizhu Yang, Runheng Zhang and Shuhan Wang conducted the research. Yinghong Tian, Yaqi Yang and Jing Liu provided technical guidance.

Acknowledgements

Not applicable.

References

1. Wang H, Liu Y, Li J, Wang T, Hei Y, Li H, Wang X, Wang L, Zhao R, Liu W, Long Q (2021) Tail-vein injection of MSC-derived small extracellular vesicles facilitates the restoration of hippocampal neuronal morphology and function in APP / PS1 mice. Cell Death Discov 7:230.
2. Goedert M, Spillantini MG (2006) A century of Alzheimer's disease. Science 314:777-781
3. (2021) 2021 Alzheimer's disease facts and figures. Alzheimers Dement 7:327-406
4. Jia L, Du Y, Chu L, Zhang Z, Li F, Lyu D, Li Y, Li Y et al (2020) Prevalence, risk factors, and management of dementia and mild cognitive impairment in adults aged 60 years or older in China: a cross-sectional study. Lancet Public Health 5: e661-e671
5. Chen Q, Kang J, Fu C (2018) The independence of and associations among apoptosis, autophagy, and necrosis. Signal Transduct Target Ther 3:18
6. Scrivo A, Bourdenx M, Pampliega O, Cuervo AM (2018) Selective autophagy as a potential therapeutic target for neurodegenerative disorders. Lancet Neurol 17:802-815
7. Li X, Lu J, Xu Y, Wang J, Qiu X, Fan L, Li B, Liu W et al (2020) Discovery of nitazoxanide-based derivatives as autophagy activators for the treatment of Alzheimer's disease. Acta Pharm Sin B 10:646-666
8. Li Q, Liu Y, Sun M (2017) Autophagy and Alzheimer's Disease. Cell Mol Neurobiol 37:377-388
9. Gao L, Li X, Meng S, Ma T, Wan L, Xu S (2020) Chlorogenic Acid Alleviates $A\beta_{25-35}$-Induced Autophagy and Cognitive Impairment via the mTOR/TFEB Signaling Pathway. Drug Des Devel Ther 14:1705-1716
10. Choi Y, Bowman JW, Jung JU (2018) Autophagy during viral infection-a double-edged sword. Nat Rev Microbiol 16:341-354
11. Yang DJ, Zhu L, Ren J, Ma RJ, Zhu H, Xu J (2015) Dysfunction of autophagy as the pathological mechanism of motor neuron disease based on a patient-specific disease model. Neurosci Bull 31:445-451
12. Chen X, Cheng C, Zuo X, Huang W (2020) Astragalin alleviates cerebral ischemia-reperfusion injury by improving anti-oxidant and anti-inflammatory activities and inhibiting apoptosis pathway in rats. BMC Complement Med Ther 20:120
13. Harikrishnan H, Jantan I, Alagan A, Haque MA (2020) Modulation of cell signaling pathways by Phyllanthus amarus and its major constituents: potential role in the prevention and treatment of

inflammation and cancer. Inflammopharmacology 28:1-18

14. Fu G, Tong H, Zeng H, Zou B, Chai J, Zhang L, Xie M, Chen F et al (2018) Antioxidant and xanthine oxidase inhibitory activity of Eucommia ulmoides Oliver leaf extracts. Pak J Pharm Sci 31:1333-1339
15. Oldoni TLC, Merlin N, Karling M, Carpes ST, Alencar SM, Morales RGF, Silva EAD, Pilau EJ et al (2019) Bioguided extraction of phenolic compounds and UHPLC-ESI-Q-TOF-MS/MS characterization of extracts of Moringa oleifera leaves collected in Brazil. Food Res Int 125:108647
16. Han XX, Jiang YP, Liu N, Wu J, Yang JM, Li YX, Sun M, Sun T et al (2019) Protective effects of Astragalin on spermatogenesis in streptozotocin-induced diabetes in male mice by improving antioxidant activity and inhibiting inflammation. Biomed Pharmacother 110:561-570
17. Zhu L, Zhu L, Chen J, Cui T, Liao W (2019) Astragalin induced selective kidney cancer cell death and these effects are mediated via mitochondrial mediated cell apoptosis, cell cycle arrest, and modulation of key tumor-suppressive miRNAs. J BUON 24:1245-1251
18. Vongsak B, Mangmool S, Gritsanapan W (2015) Antioxidant Activity and Induction of mRNA Expressions of Antioxidant Enzymes in HEK-293 Cells of Moringa oleifera Leaf Extract. Planta Med 81:1084-1089
19. Zheng D, Liu D, Liu N, Kuang Y, Tai Q (2019) Astragalin reduces lipopolysaccharide-induced acute lung injury in rats via induction of heme oxygenase-1. Arch Pharm Res 42:704-711
20. Soromou LW, Chen N, Jiang L, Huo M, Wei M, Chu X, Millimouno FM, Feng H et al (2012) Astragalin attenuates lipopolysaccharide-induced inflammatory responses by down-regulating NF-κB signaling pathway. Biochem Biophys Res Commun 419:256-261
21. Kameyama T, Nabeshima T, Kozawa T (1986) Step-down-type passive avoidance- and escape-learning method. Suitability for experimental amnesia models. J Pharmacol Methods 16:39-52
22. Zhou X, Xiao W, Su Z, Cheng J, Zheng C, Zhang Z, Wang Y, Wang L et al (2019) Hippocampal Proteomic Alteration in Triple Transgenic Mouse Model of Alzheimer's Disease and Implication of PINK 1 Regulation in Donepezil Treatment. J Proteome Res 18:1542-1552
23. Vorhees CV, Williams MT (2006) Morris water maze: procedures for assessing spatial and related forms of learning and memory. Nat Protoc 1:848-858
24. Wang C, Cai X, Wang R, Zhai S, Zhang Y, Hu W, Zhang Y, Wang D et al (2020) Neuroprotective effects of verbascoside against Alzheimer's disease via the relief of endoplasmic reticulum stress in Aβ-exposed U251 cells and APP/PS1 mice. J Neuroinflammation 17:309
25. Gao N, Liu H, Li S, Tu X, Tian S, Liu J, Li G, Ma Y et al (2019) Volatile Oil from Acorus gramineus Ameliorates the Injury Neurons in the Hippocampus of Amyloid Beta 1-42 Injected Mice. Anat Rec (Hoboken) 302:2261-2270
26. Kwon SH, Ma SX, Joo HJ, Lee SY, Jang CG (2013) Inhibitory Effects of Eucommia ulmoides Oliv. Bark on Scopolamine-Induced Learning and Memory Deficits in Mice. Biomol Ther (Seoul) 21:462-469
27. Wang K, Zhu L, Zhu X, Zhang K, Huang B, Zhang J, Zhang Y, Zhu L et al (2014) Protective effect of paeoniflorin on Aβ25-35-induced SH-SY5Y cell injury by preventing mitochondrial dysfunction. Cell

Mol Neurobiol 34:227-234

28. Yu L, Wan H, Jin W, Yang J, Li C, Dai L, Ge L, Zhou H et al (2018) Protective effects of effective ingredients of Danshen (Radix Salviae Miltiorrhizae) and Honghua (Flos Carthami) compatibility after rat hippocampal neurons induced by hypoxia injury. J Tradit Chin Med 38:685-697
29. Kong F, Jiang X, Wang R, Zhai S, Zhang Y, Wang D (2020) Forsythoside B attenuates memory impairment and neuroinflammation via inhibition on NF-κB signaling in Alzheimer's disease. J Neuroinflammation 17:305
30. Wang Y, Xu Y, Pan Y, Li W, Zhang W, Liu Y, Jia J, Li P et al (2013) Radix Achyranthis Bidentatae improves learning and memory capabilities in ovariectomized rats. Neural Regen Res 8:1644-1654
31. Rojanathammanee L, Puig KL, Combs CK (2013) Pomegranate polyphenols and extract inhibit nuclear factor of activated T-cell activity and microglial activation in vitro and in a transgenic mouse model of Alzheimer disease. J Nutr 143:597-605
32. Jiang Y, Gao H, Turdu G (2017) Traditional Chinese medicinal herbs as potential AChE inhibitors for anti-Alzheimer's disease: A review. Bioorg Chem 75:50-61
33. Uddin MS, Stachowiak A, Mamun AA, Tzvetkov NT, Takeda S, Atanasov AG, Bergantin LB, Abdel-Daim MM et al (2018) Autophagy and Alzheimer's Disease: From Molecular Mechanisms to Therapeutic Implications. Front Aging Neurosci 10:04
34. Gong Z, Huang J, Xu B, Ou Z, Zhang L, Lin X, Ye X, Kong X et al (2019) Urolithin A attenuates memory impairment and neuroinflammation in APP/PS1 mice. J Neuroinflammation 16:62
35. La Barbera L, Vedele F, Nobili A, Krashia P, Spoleti E, Latagliata EC, Cutuli D, Cauzzi E et al (2021) Nilotinib restores memory function by preventing dopaminergic neuron degeneration in a mouse model of Alzheimer's Disease. Prog Neurobiol 202:102031
36. Kosel F, Pelley JMS, Franklin TB (2020) Behavioural and psychological symptoms of dementia in mouse models of Alzheimer's disease-related pathology. Neurosci Biobehav Rev 112:634-647
37. Héraud C, Goufak D, Ando K, Leroy K, Suain V, Yilmaz Z, De Decker R, Authelet M et al (2014) Increased misfolding and truncation of tau in APP/PS1/tau transgenic mice compared to mutant tau mice. Neurobiol Dis 62:100-112
38. Gu XH, Xu LJ, Liu ZQ, Wei B, Yang YJ, Xu GG, Yin XP, Wang W et al (2016) The flavonoid baicalein rescues synaptic plasticity and memory deficits in a mouse model of Alzheimer's disease. Behav Brain Res 311:309-321
39. Denver P, English A, McClean PL (2018) Inflammation, insulin signaling and cognitive function in aged APP/PS1 mice. Brain Behav Immun 70:423-434
40. Holtzman DM, Morris JC, Goate AM (2011) Alzheimer's disease: the challenge of the second century. Sci Transl Med 3:77sr1
41. Mawuenyega KG, Sigurdson W, Ovod V, Munsell L, Kasten T, Morris JC, Yarasheski KE, Bateman RJ et al (2010) Decreased clearance of CNS beta-amyloid in Alzheimer's disease. Science 330:1774

42. Mehta PD, Patrick BA, Miller DL, Coyle PK, Wisniewski T (2020) A Sensitive and Cost-Effective Chemiluminescence ELISA for Measurement of Amyloid-β 1-42 Peptide in Human Plasma. J Alzheimers Dis 78:1237-1244
43. Li N, Zhang K, Mu X, Tian Q, Liu W, Gao T, Ma X, Zhang J et al (2018) Astragalin Attenuates UVB Radiation-induced Actinic Keratosis Formation. Anticancer Agents Med Chem 18:1001-1008
44. Li X, Tang Z, Fei D, Liu Y, Zhang M, Liu S (2017) Evaluation of the sedative and hypnotic effects of astragalin isolated from Eucommia ulmoides leaves in mice. Nat Prod Res 31:2072-2076
45. Jeong HR, Kim KJ, Lee SG, Cho HS, Cho YS, Kim DO (2020) Phenolic Profiles of Hardy Kiwifruits and Their Neuroprotective Effects on PC-12 and SH-SY5Y Cells against Oxidative Stress. J Microbiol Biotechnol 30:912-919
46. Chung MJ, Lee S, Park YI, Lee J, Kwon KH (2016) Neuroprotective effects of phytosterols and flavonoids from Cirsium setidens and Aster scaber in human brain neuroblastoma SK-N-SH cells. Life Sci 148:173-182
47. Yuan Z, Luan G, Wang Z, Hao X, Li J, Suo Y, Li G, Wang H et al (2017) Flavonoids from Potentilla parvifolia Fisch. and Their Neuroprotective Effects in Human Neuroblastoma SH-SY5Y Cells in vitro. Chem Biodivers 14:10.1002/cbdv.201600487.
48. Zhu XC, Yu JT, Jiang T, Tan L (2013) Autophagy modulation for Alzheimer's disease therapy. Mol Neurobiol 48:702-714
49. Bordi M, Berg MJ, Mohan PS, Peterhoff CM, Alldred MJ, Che S, Ginsberg SD, Nixon RA et al (2016) Autophagy flux in CA1 neurons of Alzheimer hippocampus: Increased induction overburdens failing lysosomes to propel neuritic dystrophy. Autophagy 12:2467-2483
50. Lee JH, Yu WH, Kumar A, Lee S, Mohan PS, Peterhoff CM, Wolfe DM, Martinez-Vicente M et al (2010) Lysosomal proteolysis and autophagy require presenilin 1 and are disrupted by Alzheimer-related PS1 mutations. Cell 141:1146-1158
51. Song X, Liu B, Cui L, Zhou B, Liu W, Xu F, Hayashi T, Hattori S et al (2017) Silibinin ameliorates anxiety/depression-like behaviors in amyloid β-treated rats by upregulating BDNF/TrkB pathway and attenuating autophagy in hippocampus. Physiol Behav 179:487-493
52. Golestaneh N, Chu Y, Xiao YY, Stoleru GL, Theos AC (2017) Dysfunctional autophagy in RPE, a contributing factor in age-related macular degeneration. Cell Death Dis 8: e2537
53. Li Y, Xu Y, Xie J, Chen W (2020) Malvidin-3-O-arabinoside ameliorates ethyl carbamate-induced oxidative damage by stimulating AMPK-mediated autophagy. Food Funct 11:10317-10328
54. Lamark T, Svenning S, Johansen T (2017) Regulation of selective autophagy: the p62/SQSTM1 paradigm. Essays Biochem 61:609-624
55. Sun Q, Chen X, Liu W, Li S, Zhou Y, Yang X, Liu J (2021) Effects of long-term low dose saxitoxin exposure on nerve damage in mice. Aging (Albany NY) 13:17211-17226.
56. Kihara A, Kabeya Y, Ohsumi Y, Yoshimori T (2001) Beclin-phosphatidylinositol 3-kinase complex functions at the trans-Golgi network. EMBO Rep 2:330-335

57. Mizushima N, Yoshimori T, Levine B (2010) Methods in mammalian autophagy research. Cell 140:313-326
58. Sun L, Liu A, Zhang J, Ji W, Li Y, Yang X, Wu Z, Guo J et al (2018) miR-23b improves cognitive impairments in traumatic brain injury by targeting ATG12-mediated neuronal autophagy. Behav Brain Res 340:126-136
59. Klionsky DJ, Abdelmohsen K, Abe A, Abedin MJ, Abeliovich H, Acevedo Arozena A, Adachi H, Adams CM et al (2016) Guidelines for the use and interpretation of assays for monitoring autophagy (3rd edition). Autophagy 12:1-222
60. Witte KE, Slotta C, Lütkemeyer M, Kitke A, Coras R, Simon M, Kaltschmidt C, Kaltschmidt B et al (2020) PLEKHG5 regulates autophagy, survival and MGMT expression in U251-MG glioblastoma cells. Sci Rep 10:21858
61. Bain HDC, Davidson YS, Robinson AC, Ryan S, Rollinson S, Richardson A, Jones M, Snowden JS et al (2019) The role of lysosomes and autophagosomes in frontotemporal lobar degeneration. Neuropathol Appl Neurobiol 45:244-261
62. Gurney R, Davidson YS, Robinson AC, Richardson A, Jones M, Snowden JS, Mann DMA (2018) Lysosomes, autophagosomes and Alzheimer pathology in dementia with Lewy body disease. Neuropathology 10.1111/neup.12472.
63. Yang B, Yan P, Gong H, Zuo L, Shi Y, Guo J, Guo R, Xie J et al (2016) TWEAK protects cardiomyocyte against apoptosis in a PI3K/AKT pathway dependent manner. Am J Transl Res 8:3848-3860
64. Switon K, Kotulska K, Janusz-Kaminska A, Zmorzynska J, Jaworski J (2017) Molecular neurobiology of mTOR. Neuroscience 341:112-153
65. Bi D, Yao L, Lin Z, Chi L, Li H, Xu H, Du X, Liu Q et al (2021) Unsaturated mannuronate oligosaccharide ameliorates β-amyloid pathology through autophagy in Alzheimer's disease cell models. Carbohydr Polym 251:117124
66. Zhang Z, Wang X, Zhang D, Liu Y, Li L (2019) Geniposide-mediated protection against amyloid deposition and behavioral impairment correlates with downregulation of mTOR signaling and enhanced autophagy in a mouse model of Alzheimer's disease. Aging (Albany NY) 11:536-548
67. Zhang Z, Gao W, Wang X, Zhang D, Liu Y, Li L (2020) Geniposide effectively reverses cognitive impairment and inhibits pathological cerebral damage by regulating the mTOR Signal pathway in APP/PS1 mice. Neurosci Lett 720:134749

Figures

Figure 1

Timeline of experimental design.

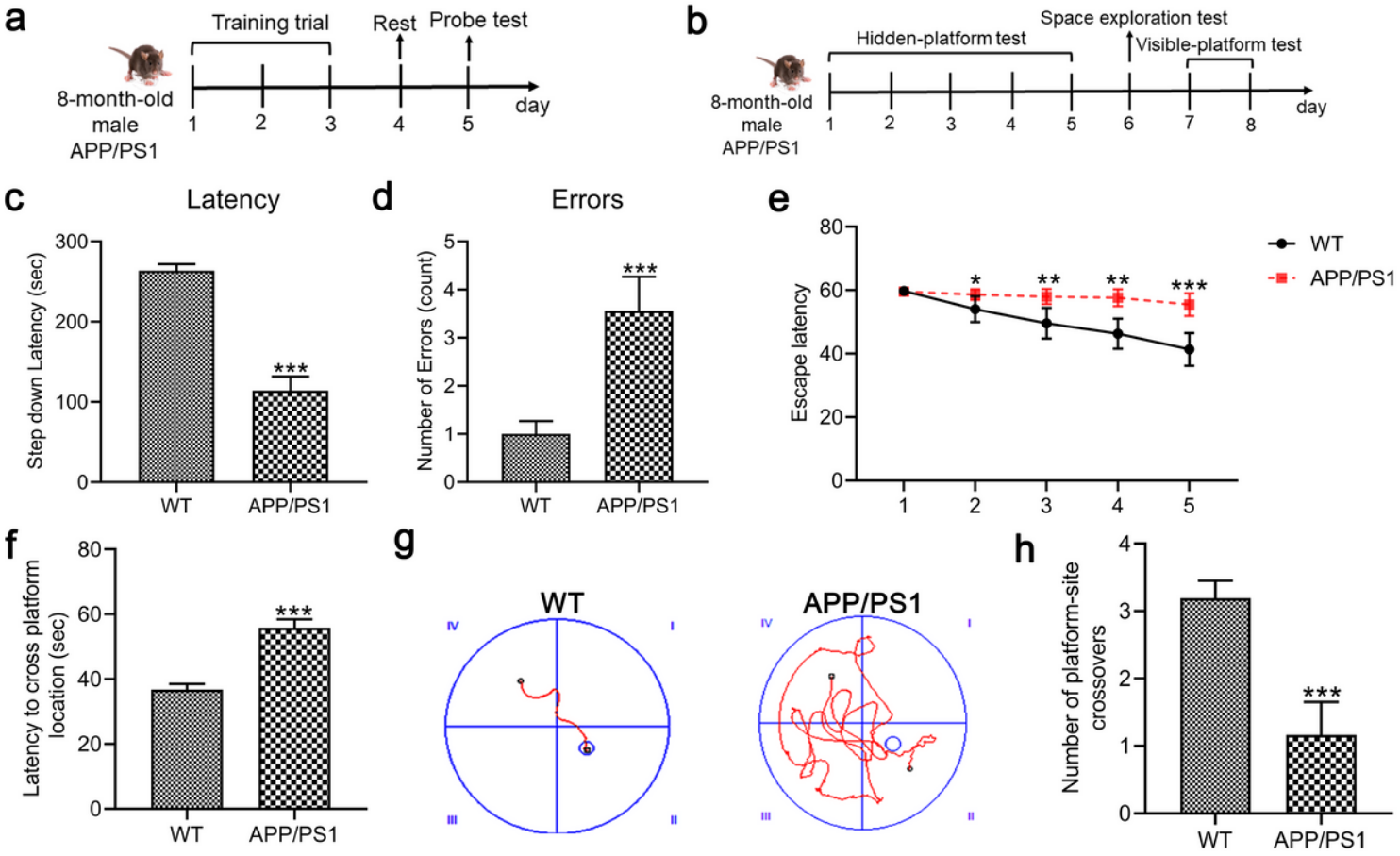

Figure 2

Cognitive capabilities of APP/PS1 mice were impaired in step-down avoidance (SDA) test and Morris water maze (MWM) test before AST treatment. (a-b) Timeline of the mouse SDA and MWM test. (c, d) The step-down latency and the number of errors of mice in SDA test. (e) The escape latency of mice to arrive at the platform during hidden-platform period in the MWM test (Day 1-5). (f) The latency of mice crossing from the starting position to the target quadrant during the space exploration in the MWM test (Day 6). (g-h) Swimming trajectory diagrams of mice and the numbers of mice crossing the target platform quadrant within 1 min during the visible platform period in the MWM test (Day 7-8). Data were presented as mean ± SD, n= 7 (WT mice), n=28 (APP/PS1 mice), $^{*}p < 0.05$, $^{**}p < 0.01$ or $^{***}p < 0.001$ *vs* WT group, two-tailed unpaired Student's *t* test and two-way ANOVA Multiple comparisons were used for statistical analysis.

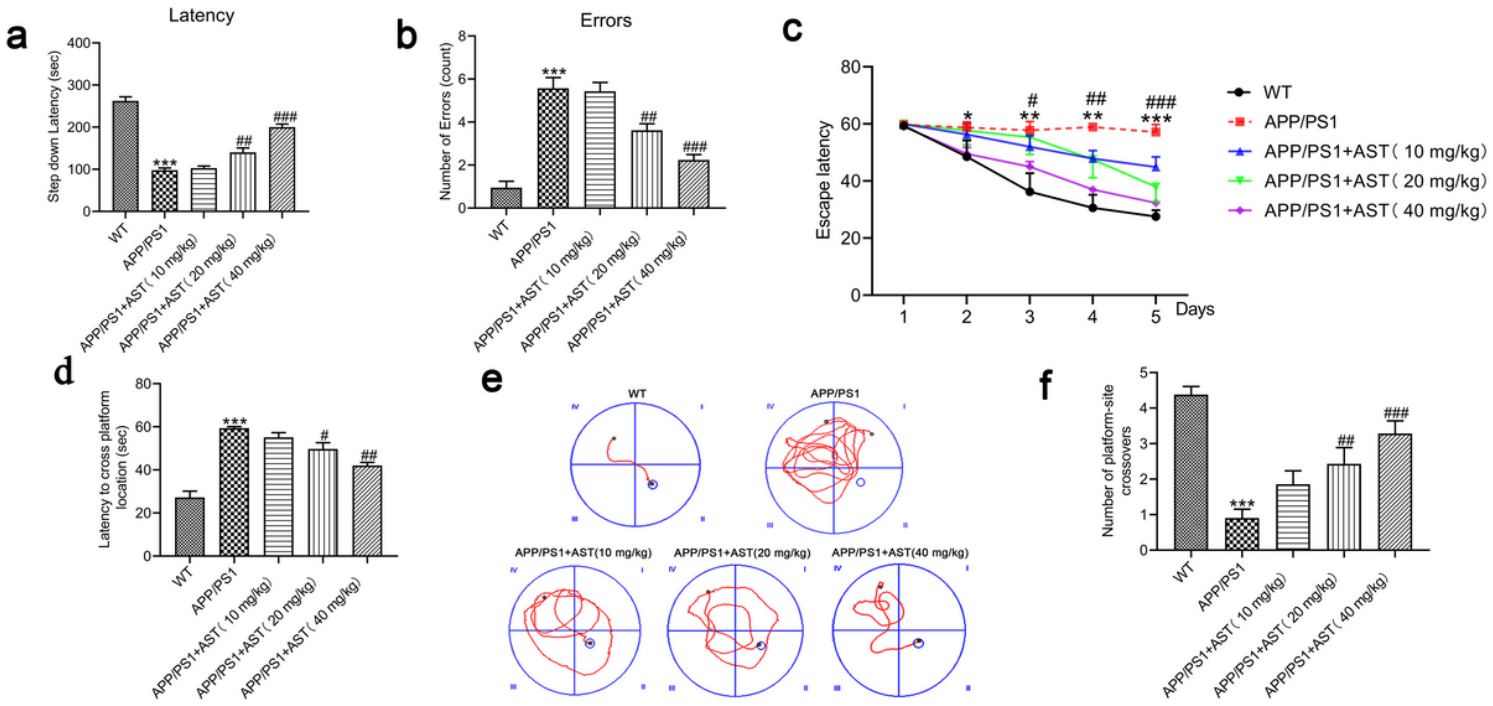

Figure 3

AST improved cognitive capabilities of APP/PS1 mice in step-down avoidance (SDA) test and Morris water maze (MWM) test. (a, b) The step-down latency and the number of errors of mice in SDA test. (c) The escape latency of mice to reach the platform during hidden-platform period in the MWM test (Day 1-5). (d) The latency of mice crossing from the starting position to the target quadrant during the space exploration in the MWM test (Day 6). (e-f) Swimming traces of mice and the numbers of mice crossing the target platform quadrant within 1 min during the visible platform period in the MWM test (Day 7-8). Data were presented as mean ± SD, n= 7 in each group, $^{*}p < 0.05$, $^{**}p < 0.01$ or $^{***}p < 0.001$ *vs* WT group, $^{\#}p < 0.05$, $^{\#\#}p < 0.01$ or $^{\#\#\#}p < 0.001$ *vs* APP/PS1 group, one-way and two-way ANOVA Multiple comparisons were used for statistical analysis.

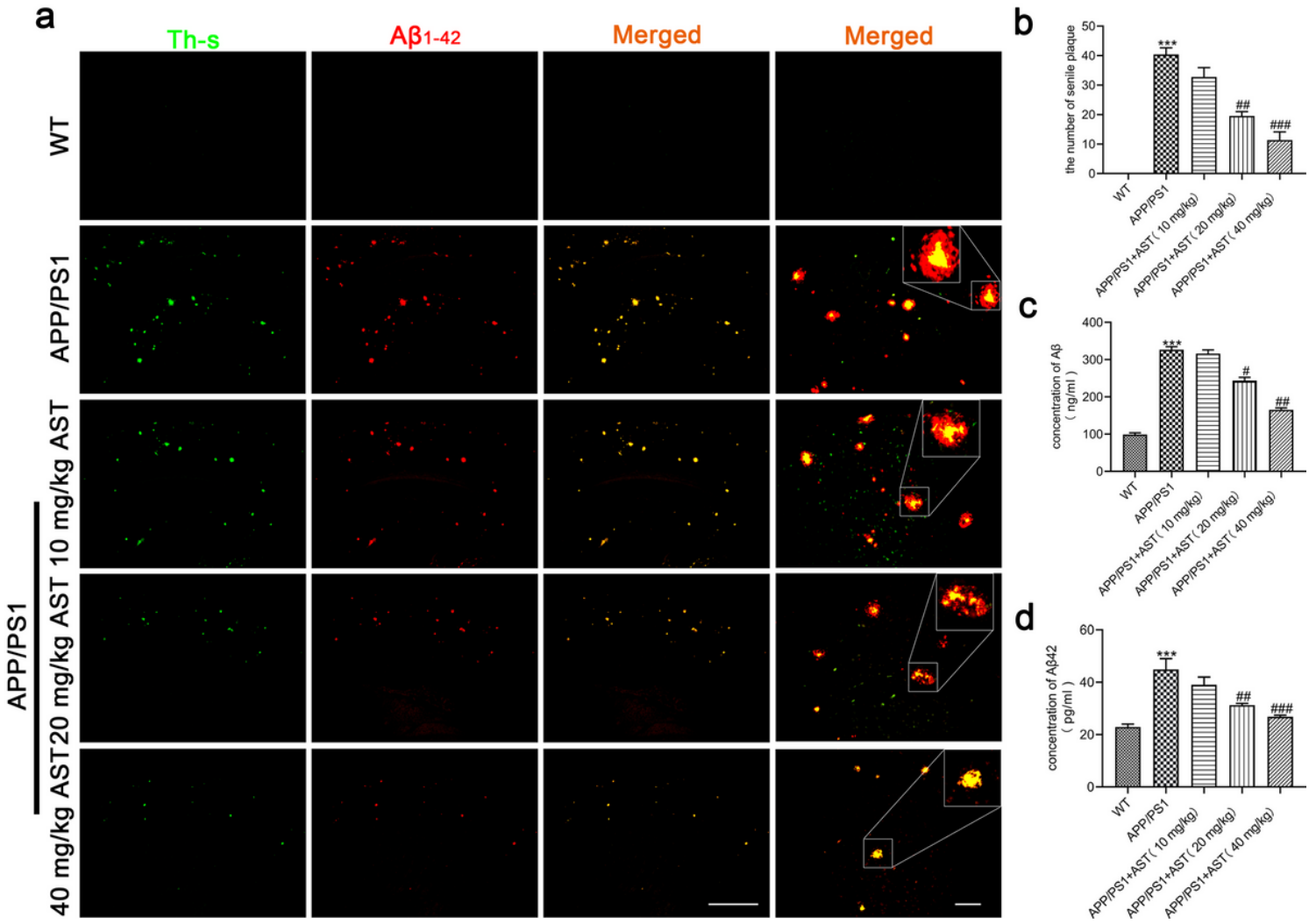

Figure 4

Astragalin reduced Aβ plaques aggregation in the brain of APP/PS1 mice and the levels of Aβ and Aβ42 in the serum of APP/PS1 mice. (a) Detection of Aβ plaques in mice brain by thioflavin S staining and immunofluorescence co-staining. (b) Statistical analysis of the number of Aβ plaques in the brain of mice. Data were presented as mean ± SD, n = 4 per group. (c-d) The Aβ and Aβ42 levels in mice serum were detected by ELISA. Data were presented as mean ± SD, n = 3 per group, $^{***}p < 0.001$ *vs* WT group, $^{\#}p < 0.05$, $^{\#\#}p < 0.01$ or $^{\#\#\#}p < 0.001$ *vs* APP/PS1 group, one-way ANOVA Multiple comparisons was used for statistical analysis.

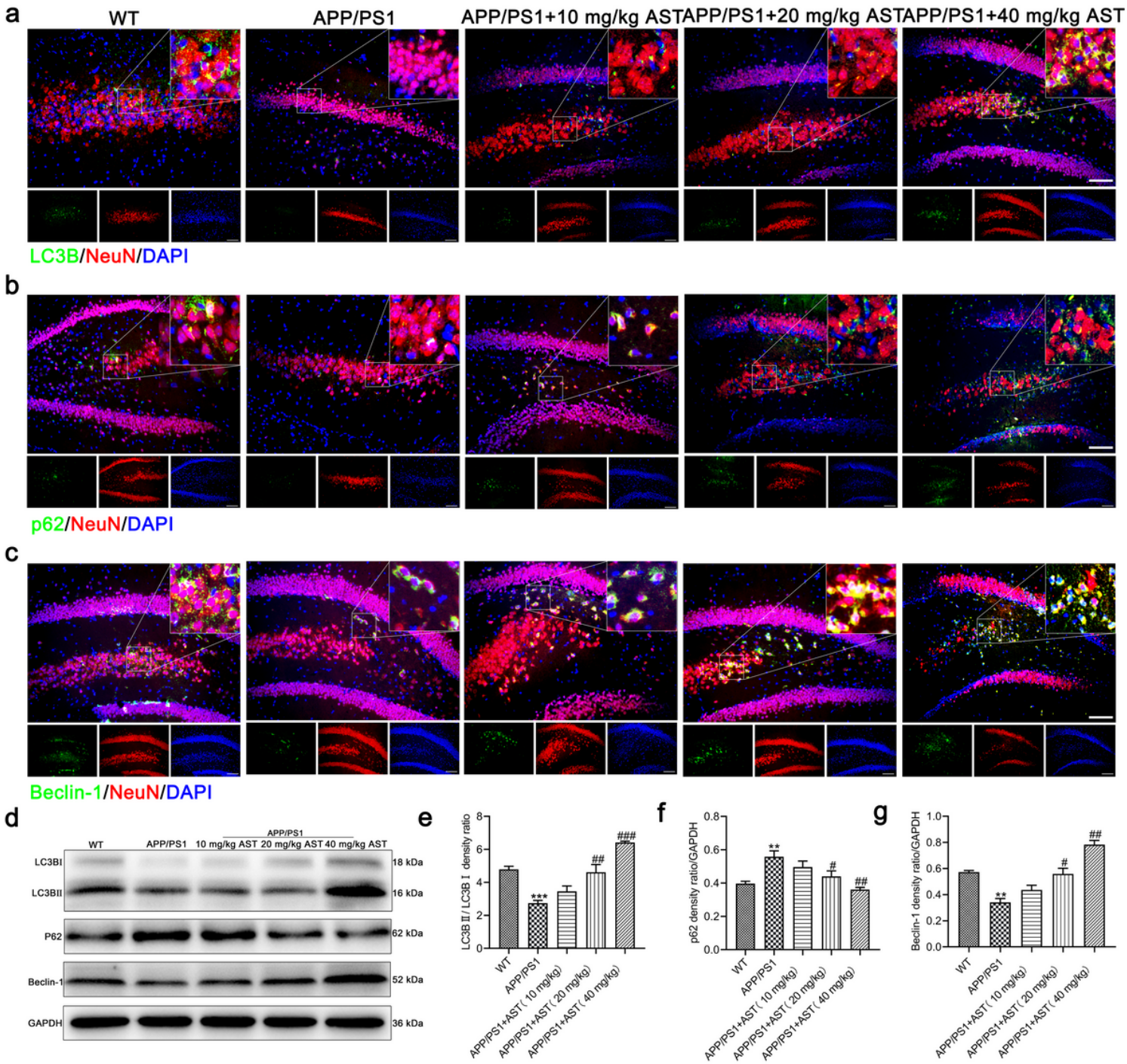

Figure 5

AST stimulated autophagy initiation in hippocampal neurons of APP/PS1 mice. (a-c) Representative immunofluorescent staining of LC3B/p62/Beclin-1, NeuN and DAPI in hippocampal neurons of mice in each group. Scale bar=100 μm, n= 4 per group. (d) Representative bands of LC3B, p62 and Beclin-1 in the hippocampus of each group by WB detection, n= 3 per group. (e-g) Statistical analysis of LC3B, p62 and Beclin-1 proteins of in hippocampus of each group. Data were presented as mean ± SD, n= 3 per group, $^{**}p < 0.01$ or $^{***}p < 0.001$ *vs* WT group, $^{\#}p < 0.05$, $^{\#\#}p < 0.01$ or $^{\#\#\#}p < 0.001$ *vs* APP/PS1 group, one-way ANOVA Multiple comparisons was used for statistical analysis.

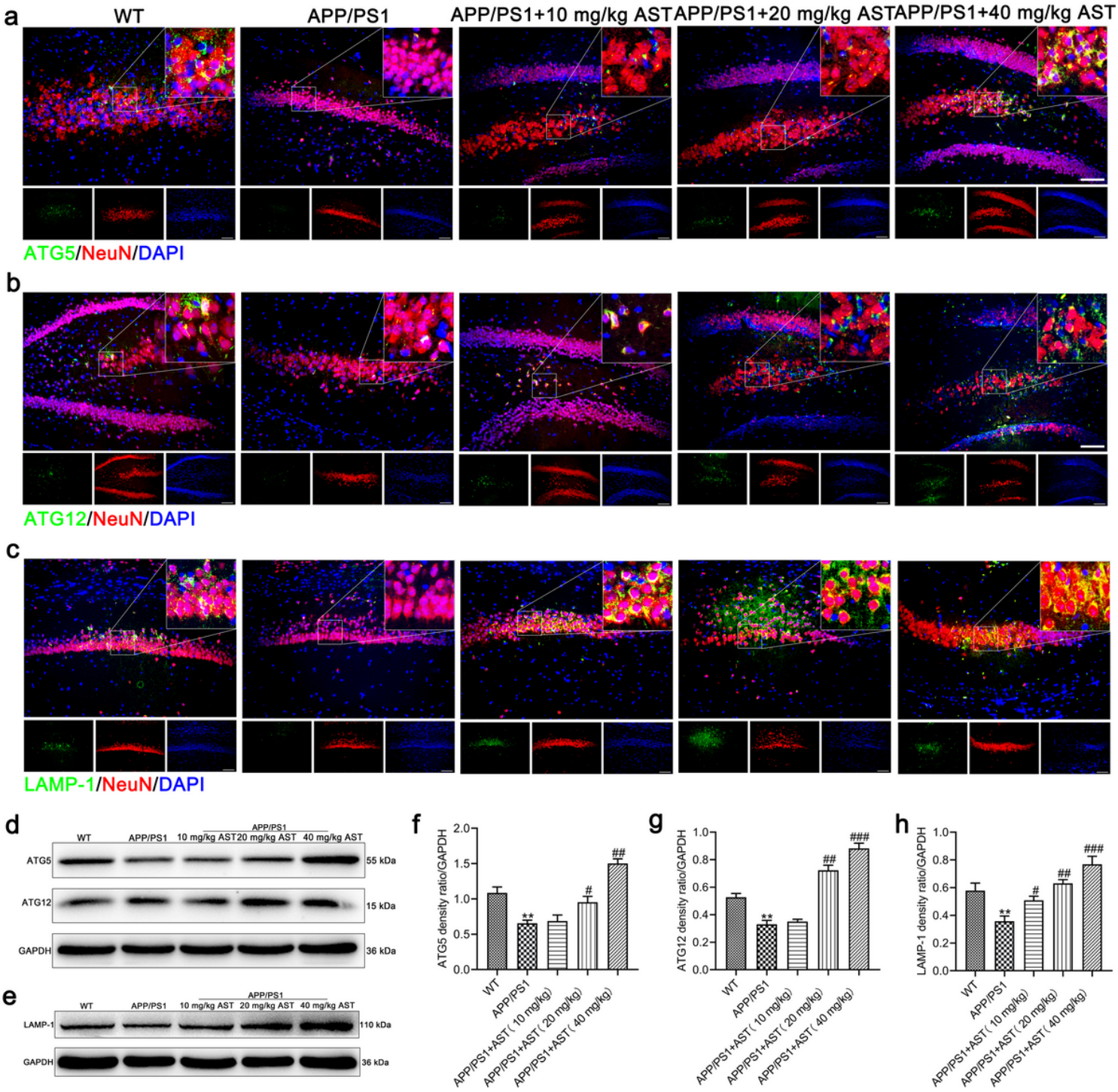

Figure 6

AST promoted autophagosome formation and the initiation of autophagic lysosomal phase in hippocampal neurons of APP/PS1 mice. (a-c) Representative immunofluorescent staining of ATG5/ATG12/LAMP-1, NeuN and DAPI in hippocampal neurons of mice in each group. Scale bar=100 μm, n= 4 per group. (d-e) Representative bands of ATG5, ATG12 and LAMP-1 in the hippocampus of each group by WB detection, n= 3 per group. (f-h) Statistical analysis of ATG5, ATG12 and LAMP-1 proteins in hippocampus of each group. Data were presented as mean ± SD, n= 3 per group, $^{**}p < 0.01$ or *vs* WT

group, $^{\#}p < 0.05$, $^{\#\#}p < 0.01$ or $^{\#\#\#}p < 0.001$ *vs* APP/PS1 group, one-way ANOVA Multiple comparisons was used for statistical analysis.

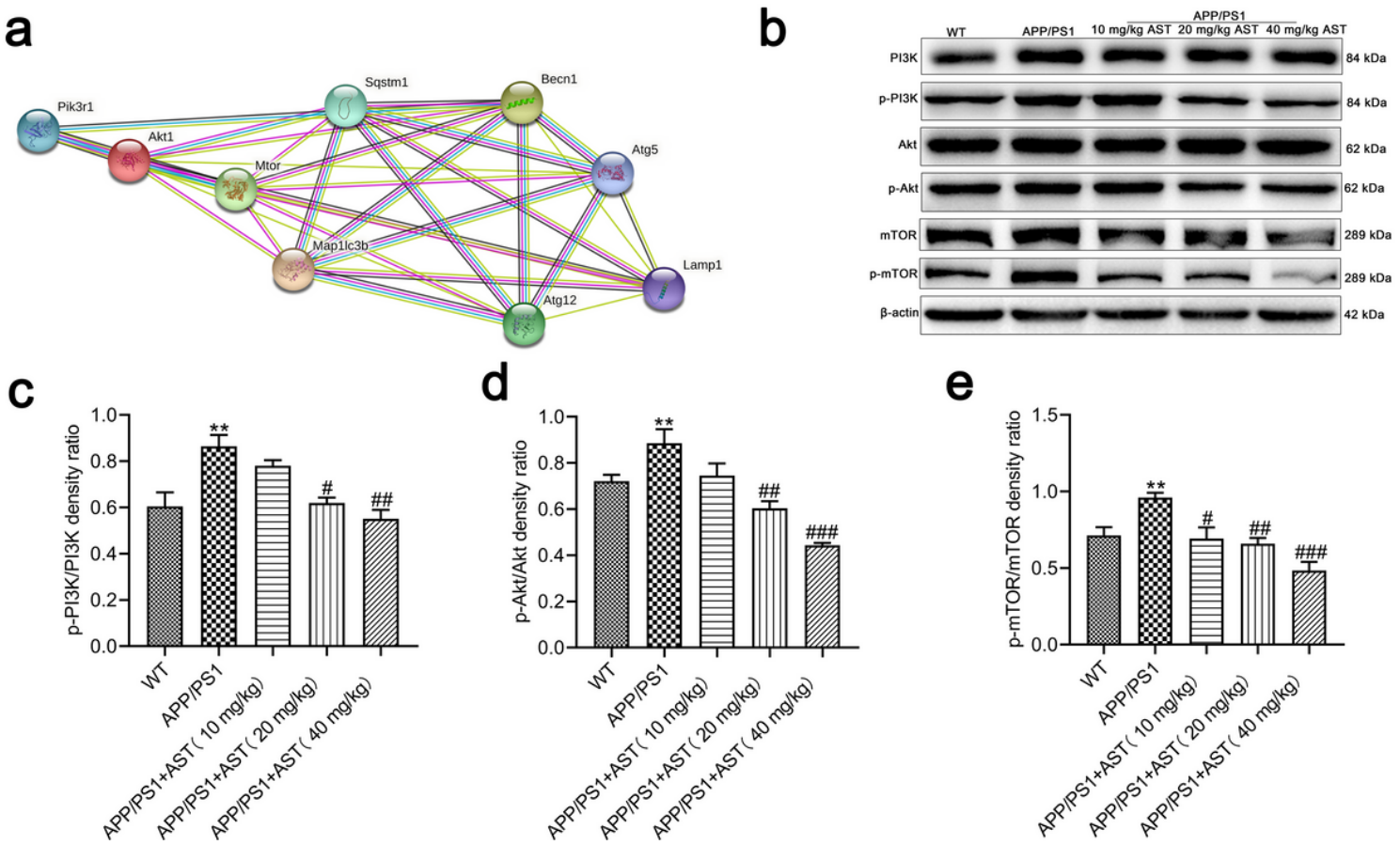

Figure 7

AST inhibited PI3K/Akt-mTOR signaling pathway in the hippocampus of APP/PS1 mice. (a) Protein-protein interaction analysis of differently expressed autophagy-associated proteins using STRING database. (b) Representative bands of PI3K, p-PI3K, Akt, p-Akt, mTOR and p-mTOR in the hippocampus of each group by WB detection. (c-e) Statistical analysis of p-PI3K/PI3K, p-Akt/Akt and p-mTOR/mTOR in mice hippocampus of each group. Data were presented as mean ± SD, n= 3 per group, $^{**}p < 0.01$ *vs* WT group, $^{\#}p < 0.05$, $^{\#\#}p < 0.01$ or $^{\#\#\#}p < 0.001$ *vs* APP/PS1 group, one-way ANOVA Multiple comparisons was used for statistical analysis.

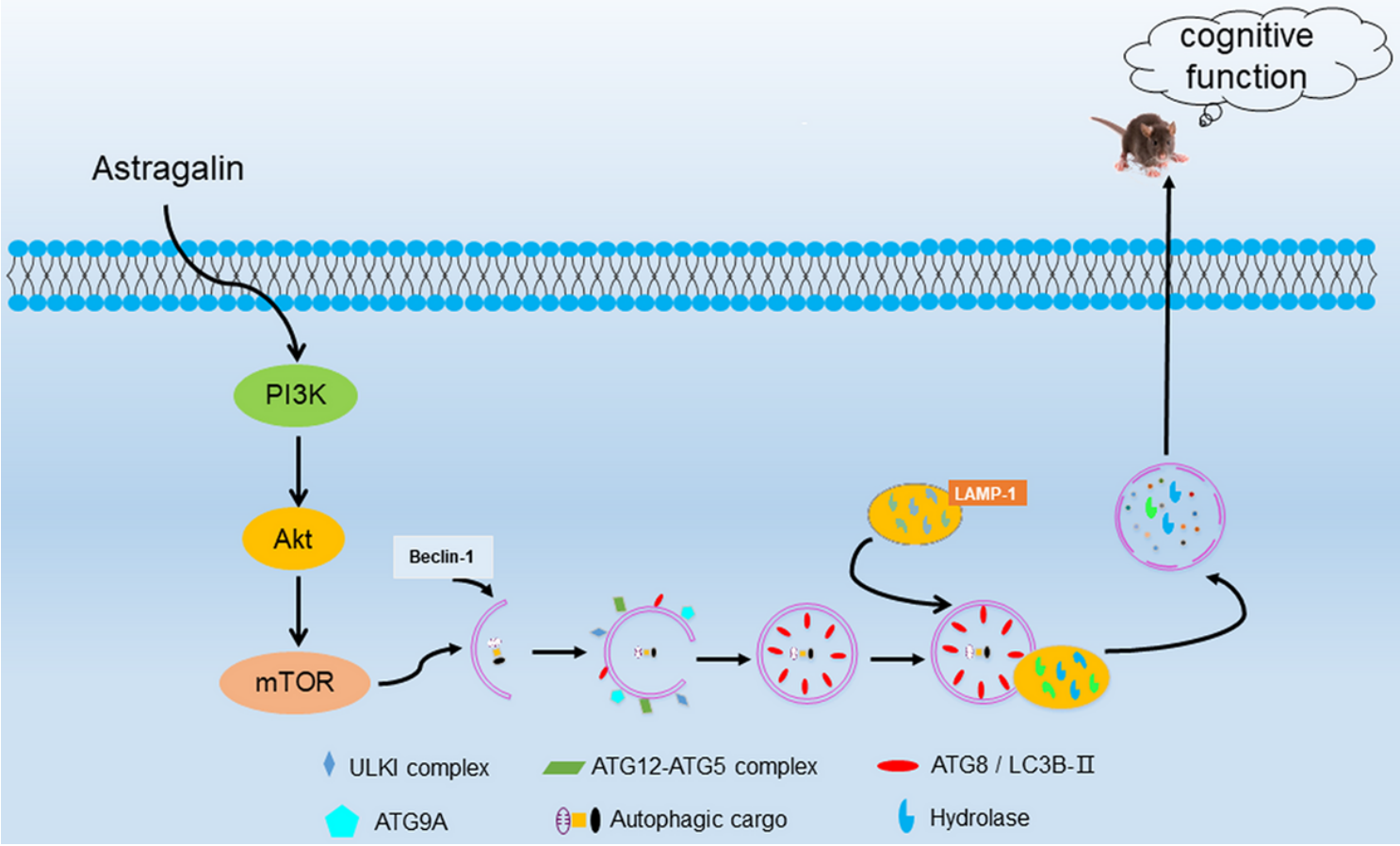

Figure 8

Relevant neuroprotective mechanism of AST in APP/PS1 mice.